

LASER THOMSON SCATTERING DIAGNOSTICS OF NON-EQUILIBRIUM HIGH PRESSURE PLASMAS

K. Muraoka^{*}, K. Uchino, M. D. Bowden and Y. Noguchi

Interdisciplinary Graduate School of Engineering Sciences, Kyushu University,
Kasuga, Fukuoka 816-8580, Japan

1 Introduction

For various applications of non-equilibrium high pressure plasmas, knowledge of electron properties, such as electron density, electron temperature and/or electron energy distribution function (eedf), is prerequisite for any rational approach to understanding physical and chemical processes occurring in the plasmas. For this purpose, laser Thomson scattering has been successfully applied for the first time to measure the electron properties in plasmas for excimer laser pumping and in microdischarges. Although this diagnostic technique is well established for measurements in high temperature plasmas, its applications to these glow discharge plasmas have had various inherent difficulties, such as a presence of high density neutral particles ($>10^{21} \text{ m}^{-3}$) in the excimer laser pumping discharges and an extremely small plasma size ($<0.1 \text{ mm}$) and the presence of nearby walls for microdischarges. These difficulties have been overcome and clear signals have been obtained. The measured results are presented and their implications in the respective discharge phenomena are discussed.

2 Excimer laser plasmas

There were several difficulties in a laser Thomson scattering experiment on an excimer pumping discharge that had to be considered before the apparatus could be designed. Firstly, it was expected that the electron density would be of the order of 10^{21} m^{-3} , much smaller than the background gas density, which is $\sim 10^{26} \text{ m}^{-3}$ at the pressures of several atmospheres that are typical for excimer lasers. Hence, Rayleigh scattering from the gas particles would be extremely large compared with Thomson scattering from the electrons. Secondly, the discharge occurs over a time of 30~40 ns, and the plasma properties vary rapidly during this period. Hence, temporal resolution of about 1 ns was desirable.

To overcome the first problem, a double monochromator with high rejection efficiency was used. The Rayleigh scattered light appears only at the laser wavelength whereas the Thomson scattered spectrum is broadened by the Doppler motion of the electrons. Use of the double monochromator reduced the effect of the Rayleigh signal on the measurement of the Thomson spectrum. The second problem was dealt with by using a YAG laser with sub-nanosecond pulse width to measure with good temporal resolution.

The apparatus used for the experiment that used the sub-nanosecond laser is shown in figure 1. The excimer laser discharge studied in this experiment had a chamber with length 800 mm, width 400 mm and height 560 mm. The distance between the electrodes was 20 mm.

The sub-nanosecond laser source was a Q-switched YAG laser with active mode-locking and two amplifier stages. A second-harmonic-generation crystal was used to generate light at 532 nm for the scattering experiment. The laser output had a pulse width of 0.3 ns and an energy of 300 mJ. The beam from the YAG laser was sent along the excimer laser axis, and the scattered light was collected perpendicularly to the laser beam direction by a lens that had focal length of 300 mm. A viewing dump and light baffles were used to reduce the amount of stray laser light entering the detection system. The scattered light was dispersed by the double monochromator, whose output was sent via optical fibre bundles to a photomultiplier. The output of the photomultiplier was displayed on a digital oscilloscope and then transferred to a computer. The double monochromator had a theoretical rejection of about 10^{-9} , where rejection is defined quantitatively as

^{*} Author to whom correspondence should be addressed.

the ratio of the transmitted light intensity at the set wavelength. Although the actual rejection in an experiment is lower than this theoretical value, the rejection of the double monochromator is extremely good compared with the rejection of 10^{-4} of most single stage devices. Hence, this spectrometer was ideally suited to this scattering experiment.

The temporal response of the photomultiplier was very important because the Thomson scattering signal generated by the YAG laser also was in the form of a short pulse. For this reason, a photomultiplier incorporating a microchannel plate (Hamamatsu R2024U), with response of 0.3 ns, was used. The oscilloscope used to view and digitize the signal was a Sony-Textronix MP1101 model, with temporal response of 0.53 ns.

Figure 2 is an example of a measured spectrum, showing the intensity of scattered signals measured at different wavelengths. For this measurement, the laser was operated in a gas mixture of Kr/F/Ne with pressures of 30 Torr/1.5 Torr/3 atm, which is a standard gas mix for a KrF laser. The measured spectral points could be fitted with a straight line (on this graph with axes of $(\Delta\lambda)^2$ and $\log(\text{signal})$), and this indicated that $f(v_e)$ was a Maxwellian distribution. A numerical simulation of the discharge for these conditions predicted that $f(v_e)$ would be a non-Maxwellian function [1]. This result is shown by the thin line in figure 2. The measurements, however, indicated that $f(v_e)$ was, in fact, a Maxwellian distribution, and so the model used for the simulation was altered to take into account electron-electron collisions, which had been neglected previously. The results of the newer simulation are shown in figure 2 by the thick solid line, and agree satisfactorily with the measurements.

From the spectrum shown in figure 2, T_e was determined to be $(2.7 \diamond 0.4)$ eV, and from the total Thomson scattered signal intensity, the electron density was determined to be $n_e = (1.8 \diamond 0.2) \star 10^{21} \text{ m}^{-3}$. Electron density and temperature were measured in this way at different times throughout the pulse of the excimer laser discharge. An example of these results is shown in figure 3 together with the results of simulations of the discharge. The time shown on the horizontal axis represents the time from the trigger of the excimer laser's thyratron switch. The plotted points are the average of the data from 10 laser shots and the error bars were determined by the scatter of the data. The results of the two simulations, one that neglected electron-electron collisions and one that included these collisions, also are shown. The simulation that neglected electron-electron collisions predicted that $f(v_e)$ was non-Maxwellian, and so the results for this case show the average electron energy, rather than the electron temperature. From figure 3, it is clear that the measured electron density agreed much better with the results of the simulation that included electron collisions. The electron temperatures predicted by both simulations are within the experimental errors.

Measurements such as these were performed for different gas mixtures and different gas pressures. These results allowed the simulation of the discharge to be improved by comparing its predictions with experimental results. This led to better quantitative understanding of phenomena occurring in discharge-pumped excimer lasers.

Presently, this technique is being employed for further improvement of actual discharge pumped excimer lasers used for lithography.

3 Microdischarge plasmas

In the application of Thomson scattering to microdischarge plasmas, two main difficulties were anticipated. The first of these is that the size of the plasmas is about 0.1 – 1 mm, and so the linear dimension of the scattering volume should be around or less than 0.1 mm. This means that the Thomson scattering signal is very small. The second difficulty is that the stray laser light becomes very strong because the wall of the discharge cell is very close to the scattering volume. Also, the Rayleigh scattering intensity is strong due to high gas pressure. In order to consider the second problem, we calculated the degree of stray light suppression that is necessary. For the case that the stray light level in the actual experiment was equivalent to the Rayleigh scattering intensity from argon gas at a pressure of 1000 Torr, we calculated that we needed a spectrometer whose stray light rejection was 10^{-7} at the differential wavelength of $\Delta\lambda = 1 \text{ nm}$ from the laser wavelength. In order to meet this requirement, we fabricated a special spectrometer, called a triple-grating spectrometer (TGS).

Figures 4(a) and 4(b) show schematic diagrams of experimental apparatus and electrodes configuration, respectively. The apparatus consists of a discharge chamber, an electrode substrate with a driving circuit, laser input optics, and a detection system.

The discharge chamber housed the electrode substrate and some baffles for reducing the laser stray light level. The electrodes shown in figure 4(b) were printed on the glass substrate whose size was $5 \times 25 \text{ mm}^2$. The electrodes were covered with SiO_2 and MgO layers with thicknesses of 15 μm and 0.5 μm , respectively.

The discharge pulses were generated by a driving voltage that had a peak of about 300 V, a frequency of 10 kHz and a duty ratio of 0.5.

The laser was the second harmonic beam of a Nd:YAG laser with a pulse width of 10 ns. The laser beam was focused above and at the center of the electrodes after it had passed through the lens (focal length $f = 200$ mm) and an input window of the chamber. The size of the focal spot was estimated to be 0.12 mm. In the present experiment, the injected laser energy into the plasma was limited to 10 mJ, in order to have the similar laser power density as for the previous experiments [2]. The distance, Z , between the laser beam path and the plane of electrodes is indicated by Z . The laser beam passed through the output window into a beam dump, which was located outside of the chamber. The output light from the TGS was converted to an electric signal using a photomultiplier tube (Hamamatsu, R1333), and then analyzed with a photon counter (Stanford Research Systems Inc., SR430).

We first examined the rejection of the TGS. The result indicates from the foregoing discussion that we could tolerate a laser stray light level of 10,000 Torr of argon gas.

In the arrangement shown in figure 4(b), the stray laser light became progressively larger as the laser beam became closer to the electrodes (i.e. as Z approached zero). At the present time, we achieved a stray light level of below 10,000 Torr of argon gas at $Z = 0.2$ mm using an optimized arrangement of baffles housed in the chamber. This result indicates that we have demonstrated the applicability of laser Thomson scattering to microdischarge plasmas. In the subsequent experiments, $Z = 0.3$ mm was chosen, in order to see the dynamic range of the measurable electron density of this laser Thomson scattering system.

Figure 5 shows Thomson scattering signals at $\Delta\lambda = 1.0 - 2.5$ nm at the longer wavelength side of the laser wavelength (532 nm) at $t = 0.85$ μ s. From the straight line of the spectrum, we see that the electron energy distribution function (eedf) was Maxwellian, and by taking the deconvolution of the instrumental width into account, we obtained an electron temperature T_e of $1.4 (\pm 0.4)$ eV. The Rayleigh scattering calibration of the whole optical system gave the electron density n_e as $8.9 (\pm 1.8) \times 10^{18}$ m^{-3} .

Figure 6 shows the temporal evolution of T_e and n_e when the timing of the incident laser relative to the discharge was changed, and the experimental conditions were kept constant. From this figure, we see that T_e peaked and decayed more rapidly than n_e . However, these details, together with the implications of the measured values of T_e and n_e , will be discussed after more thorough measurements, made at various locations and times within the discharge.

We thoroughly discussed whether the measured signal was a genuine Thomson signal from the microdischarge plasma and found that it was so [3].

Computer simulations of micro-discharge plasmas in PDP cells predict that the electron density of the plasma is in the range of $10^{17} - 10^{19}$ m^{-3} [4,5]. Hence, this method should be readily applicable for direct measurement of T_e and n_e in a micro-discharge plasma in a PDP cell. Such studies are underway to elucidate otherwise inaccessible plasma phenomena by a collaboration with a numerical simulation group.

3 Summary

We have successfully applied the laser Thomson scattering technique for the first time to obtain electron density, electron temperature and eedf of non-equilibrium high pressure plasmas for excimer laser pumping and microdischarges. It looks almost impossible to obtain these quantities by other means. It is the authors' conviction that by proper choices of laser sources, optical arrangements and instruments and detectors, it should be possible to obtain these electron properties for other various plasmas, at non-equilibrium or equilibrium conditions and at high or low pressures.

This work was conducted at the Institute for Ionized Gas and Laser Research at Kyushu University.

References

- [1] M. Maeda, A. Takahashi, T. Mizunami and Y. Miyazoe : Jpn. J. Appl. Phys. **21** (1982) 1161.
- [2] K. Muraoka, K. Uchino and M. D. Bowden : Plasma Phys. Control Fusion (UK) **40** (1998) 1221.
- [3] Y. Noguchi, A. Matsuoka, M. D. Bowden, K. Uchino and K. Muraoka : Jpn. J. Appl. Phys. (Accepted for publication).
- [4] J. Meunier, Ph. Belenger and J. P. Boeuf : J. Appl. Phys. **78** (1995) 731.
- [5] S. Rauf and M. J. Kushner : J. Appl. Phys. **85** (1999) 3460.

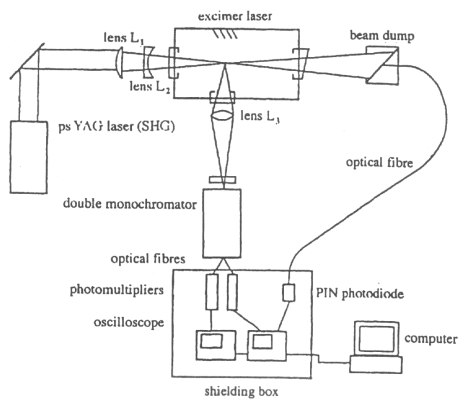


Figure 1 Arrangement for a Thomson scattering measurement in the plasma of a discharge-pumped excimer laser.

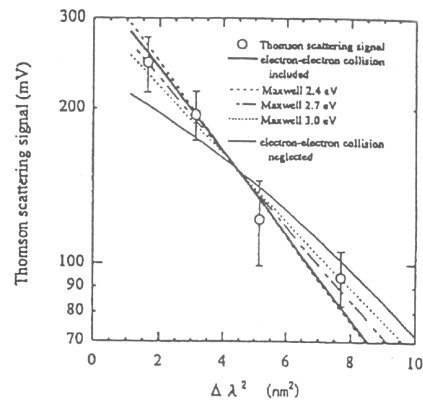


Figure 2 Thomson scattering spectra for a gas mixture of Kr/F₂/Ne=30 Torr/1.5 Torr/3 atm.

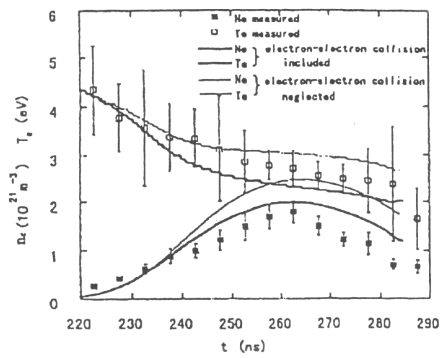


Figure 3 Temporal evolutions of electron temperature T_e and electron density n_e for a gas mixture of Kr/F₂/Ne=30 Torr/1.5 Torr/3 atm.

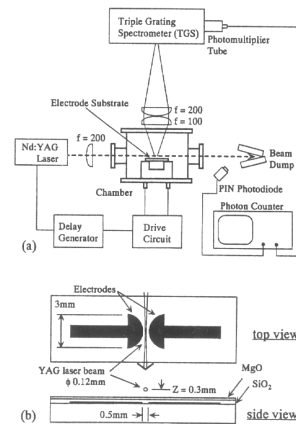


Figure 4 Schematic arrangement of (a) the experimental apparatus, together with (b) the electrodes configuration and the measurement point.

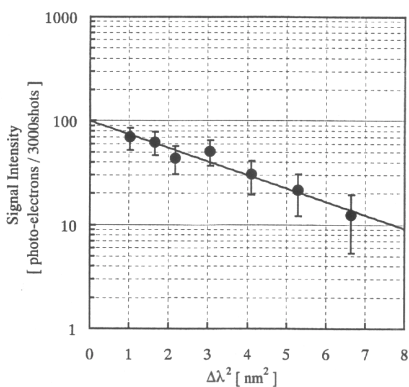


Figure 5 Thomson Scattering spectrum at an argon pressure of 50 Torr, Z=0.3 mm and t=0.85 μ s.

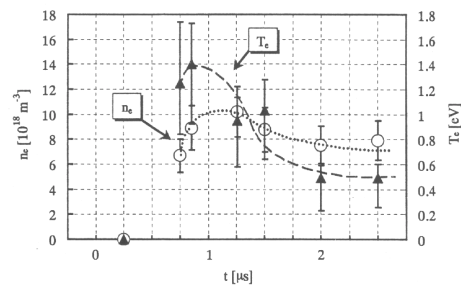


Figure 6 Temporal variation of T_e and n_e at an argon pressure of 50 Torr and Z=0.3 mm.